2024 IEEE 14th International Conference on Electronics Information and Emergency Communication (ICEIEC) | 979-8-3503-6189-6/24/$31.00 ©2024 IEEE | DOI: 10.1109/ICEIEC61773.2024.10561695

Low-overlap Crop Point Cloud Registration Method based on Improved GeoTransformer with Normal Vectors and Gaussian Curvature

Zeyuan Huang, Genping Zhao, Xiaoman Cui
School of Computer Science
Guangdong University of Technology
Guangzhou, China
1296058027@qq.com

Abstract—**Crop point cloud registration holds significant importance in measuring and monitoring crop phenotypic features. However, the 3D representation of crops differs from that of indoor or urban scenes due to the pronounced curvature of their trunks, branches, and other components, resulting in lower overlap rates between point clouds. To address this issue, we leverage the discernible normal vectors and curvature features of crops and propose a Gaussian curvature-based enhancement to GeoTransformer for aligning plant point clouds with low overlap rates. This enhancement encodes the geometric attributes of the point cloud. To assess the method's effectiveness, we conducted experiments using real-world data. The proposed method achieves RMSE errors ranging from only 1.7% to 3.8%, 6% to 28.7%, and 28.2% to 51% of those of ICP, Predator, and GeoTransformer, respectively, for low overlap rates (20%) and average values.**

Keywords-crop point cloud registration; low-overlap; normal vectors; gaussian curvature; GeoTransformer

I. INTRODUCTION

With the rapid advancement of high-precision sensors such as LiDAR and Kinect, point clouds have emerged as the primary data format for characterizing the 3D environment [1]. Given that sensors are constrained to scanning within a limited field of view for data acquisition, point cloud registration becomes essential for constructing a comprehensive 3D scene. Specifically, in the context of plants, point cloud registration holds significance for phenological measurements and monitoring of phenotypic characteristics [2]. The point cloud encapsulates the geometric structure and morphological attributes of the object, rendering it conducive for extracting plant phenotypic features. These features play a crucial role in providing insights into and monitoring the growth condition of plants.

Studies on point cloud registration for plants have been conducted. For instance, Liu et al. [3] employed two Kinect v2 sensors symmetrically positioned on both sides of a peanut plant and aligned the acquired point clouds using the geometric relationship between the sensors. Although this method effectively reconstructs and aligns the plant's morphological structure, it necessitates two acquisition devices and pre-recorded geometric relationships between them. Xie et al. [4] proposed an alignment method based on combined ISS-LCG feature points to achieve high-precision and high-efficiency automated alignment of mature oilseed rape plants, albeit under controlled conditions. Additionally, Zhu et al. [5] proposed a rapid reconstruction and alignment method for tomato canopy models using ISS-ICP and 3D-NDT. However, most existing plant point cloud registration methods are suited for scenarios with high overlap rates. Nevertheless, in real-world applications, achieving accurate registration in scenarios with low overlap rates remains challenging. Generally, the lower the overlap rate of the point cloud, the poorer the alignment effect. The traditional method, Iterative Closest Point (ICP) [6], is a well-established point cloud registration method, but its effectiveness diminishes significantly in low overlap rate scenarios. Recently, advanced point cloud registration algorithms tailored for low overlap rates in indoor and urban scenes, such as Predator [7], GeoTransformer [8], and others, have shown considerable improvements compared to methods like 3Dmatch, and they also exhibit some effectiveness in plant point cloud registration scenarios. However, considering the distinctive normal vector and curvature characteristics of plants, we propose an enhanced GeoTransformer for low overlap rate plant point cloud registration based on Gaussian curvature [9] estimated from the normal vectors of neighboring points. The key highlights of this work are summarized as follows:

(1) We propose an enhanced GeoTransformer method for point cloud registration, leveraging Gaussian curvature estimated from normal vectors of neighboring points. This method ensures rotational invariance to the point cloud and yields more precise results, particularly in scenarios involving low overlap rates in plant point cloud registration.

(2) A series of alignment experiments conducted on real-world crop point clouds acquired using a LiDAR scanner showcase the effectiveness of the proposed method.

II. IMPROVED PLANT POINT CLOUD REGISTRATION METHOD BASED ON CURVATURE AND GEOTRANSFORMER

Global context plays a pivotal role in numerous computer vision tasks, prompting the adoption of transformers to harness global contextual information for point cloud registration [10]. However, existing methods typically encode high-level features of the point cloud rather than its geometric structural features for feeding into the Transformer for learning. Although the recent

979-8-3503-6189-6/24/$31.00©2024 IEEE

GeoTransformer model, tailored for low-overlap scenes, encodes some geometric structural features of point clouds and achieves satisfactory results in indoor and urban point cloud scenes, it fails to incorporate normal vector and curvature features, rendering it less effective in plant point cloud scenes with prominent curvature features. Hence, we propose an enhanced point cloud alignment method based on curvature and GeoTransformer to enhance applicability in plant point cloud alignment scenarios with low overlap rates. This process is shown in Fig. 1. (1) Acquisition and preprocessing of point cloud data. (2) Encoding of geometric features of the point cloud, including pair-wise distances, triplet-wise angles, and point curvatures. (3) Integration and embedding of geometric feature encoding into GeoTransformer's geometric self-attention module. (4) Employment of the improved GeoTransformer for correspondence and transformation estimation.

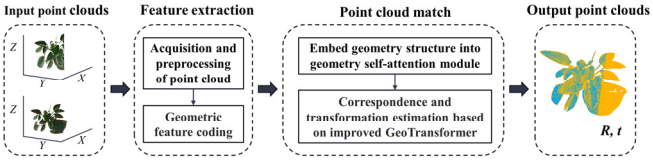

Figure 1. The workflow of the improved plant point cloud alignment method with low overlap rate

A. Point Cloud Data Acquisition and Preprocessing

The point cloud data utilized in this experiment was gathered from two potted plants on campus using a LiDAR scanner (FARO Focus s70). The acquisition protocol involved employing the LiDAR scanner to capture point clouds of the potted plants from two distinct angles (approximately 30° apart), followed by segmenting them using FARO SCENE 3D point cloud software to obtain the source and target point clouds with varying degrees of overlap. The distinct source and target point clouds are depicted in Fig. 2, while the corresponding overlap rates are presented in Table I.

However, this process typically introduces outliers stemming from unavoidable background and sensor-generated noise acquired during acquisition, which can lead to point cloud misalignment and alignment failures. To mitigate this issue, background removal and noise reduction are imperative. Specifically, the target plants were extracted from the original point cloud using FARO SCENE 3D point cloud software, and outliers were subsequently eliminated via a statistical filtering method based on Gaussian distribution.

TABLE I. OVERLAP RATES OVERLAP RATE BETWEEN TARGET AND SOURCE POINT CLOUDS

Plant-1					
Source Point Cloud	**#1**	**#2**	**#3**	**#4**	**#5**
Overlap Rate(%)	~90	~80	~60	~40	~20
Plant-2					
Source Point Cloud	**#6**	**#7**	**#8**	**#9**	**#10**
Overlap Rate(%)	~90	~80	~60	~40	~20

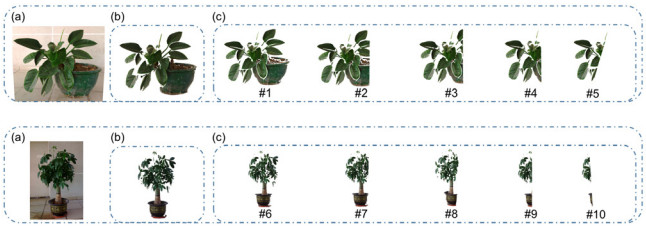

figure 2. The target and source point clouds for plant 1 and plant 2: (a) the actual scene photo of plant; (b) target point cloud; (c) source point clouds with different overlap rates with the target point cloud;

B. Point Cloud Geometric Feature Encoding and Geometric Structure Embedding

Before the point cloud correspondence estimation, the geometric features of the point cloud are encoded, including pair-wise distances $g_{i,j}^{D}$, triplet-wise angles $g_{i,j}^{A}$, and point curvatures g_i^k estimated based on normal vectors of neighboring points. Then as shown in Fig. 3, we integrate them to form a geometric structure encoding $g_{i,j}$:

$$g_{i,j} = g_{i,j}^{D} W^{D} + g_{i,j}^{A} W^{A} + g_i^k W^k, \tag{1}$$

where $W^D, W^A, W^K \in R^{d_t \times d_t}$ are the projection matrices of the pair-wise distance, triplet-wise angle, and point curvature, respectively.

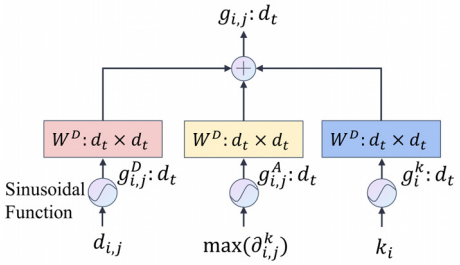

Figure 3. Encoding of the geometric structure of the point cloud

Given two points p_i and p_j in a point cloud P, based on parity position encoding, the geometric features of the point cloud are encoded as follows:

$$\begin{cases} g_{i,j,2x}^{D} = \sin\left(\dfrac{d_{i,j}/\sigma_d}{10000^{2x/d_t}}\right) \\ g_{i,j,2x+1}^{D} = \cos\left(\dfrac{d_{i,j}/\sigma_d}{10000^{2x/d_t}}\right) \end{cases}, \tag{2}$$

$$\begin{cases} g_{i,j,2x}^{A} = sin\left(\dfrac{max\left(\partial_{i,j}^k\right)/\sigma_\partial}{10000^{2x/d_t}}\right) \\ g_{i,j,2x+1}^{A} = cos\left(\dfrac{max\left(\partial_{i,j}^k\right)/\sigma_\partial}{10000^{2x/d_t}}\right) \end{cases}, \tag{3}$$

$$\begin{cases} g_{i,2x}^{k} = \sin\left(\dfrac{k_i/\sigma_k}{10000^{2x/d_t}}\right) \\ g_{i,2x+1}^{k} = \cos\left(\dfrac{k_i/\sigma_k}{10000^{2x/d_t}}\right) \end{cases}, \tag{4}$$

where $d_{i,j} = \| p_i - p_j \|_2$, $\partial_{i,j}^k = \angle(\Delta_{k,i}, \Delta_{i,j})$, $\Delta_{k,i} := p_k - p_j$, $k = 1, 2, 3$, p_k is the nearest point of point p, k_i is the Gaussian curvature of point p_i estimated based on the normal vectors of neighboring points (the computation of Gaussian curvature is illustrated below), σ_d, σ_∂, σ_k are the temperature to control the sensitivity to distance, angular and curvature variantions, and d_t is the dimension of the feature, $x = 0, 1, 2 \dots d_t/2$. The point curvatures in $\hat{Q}$ are calculated in the same way.

Gaussian curvature, as a quantity that describes the concave and convex nature of a surface, changes as the surface concavity changes, and is well suited in plant point cloud alignment scenarios where curvature is a distinctive feature. To find the Gaussian curvature based on the normal vectors of neighboring points, a normal section circle is constructed and the normal curvature is estimated based on the positions and normal vectors of two points (the target point and one of its neighbors), and then the principal curvature is found based on the relationship between the normal curvature and the principal curvature in the Euler's formula, and then the Gaussian curvature is further derived from the principal curvature.

For each point p in the point cloud, let the unit normal vector of point p be N, q_i be the ith nearest neighbor of point p, $i = 1, 2 \dots, m$, and the normal vector of q_i be M_i. Let the orthogonal coordinate system $\{p, X, Y, N\}$ be the local coordinate system L of point p, in which $p = (0, 0, 0)$, $N = (n_{x,p}, n_{y,p}, n_{z,p})$, $q_i = (x_i, y_i, z_i)$, $M_i = (n_{x,i}, n_{y,i}, n_{z,i})$, $X = (-\sin\varphi, \cos\varphi, 0)$, $\psi = arccos(n_{z,p})$, $\varphi = arctan(n_{y,p}/n_{x,p})$, $Y = (\cos\psi\cos\varphi, \cos\psi\sin\varphi, -\sin\psi)$. Fig. 4 illustrates their relationship.

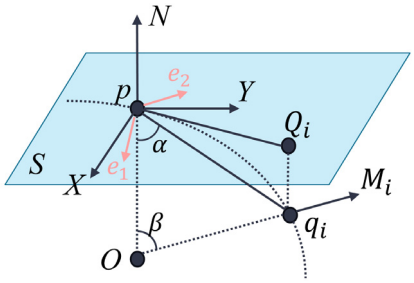

Figure 4. Local coordinate system $L = \{p, X, Y, N\}$ at point p

Then the normal curvature of p with respect to q_i is

$$k_n^i = -\frac{\sin\beta}{|pq_i|\sin\alpha}, \tag{5}$$

where α is the Angle between vectors $-N$ and pq_i, and β is the Angle between vectors N and M_i.

Let S be the plane passing through the point p and with normal vector N. The vectors e_1 and e_2 are the principal directions of the point p, corresponding to the principal curvatures k_1 and k_2, θ is the angle between the vectors e_1 and e_2, θ_i is the angle between the vectors X and pQ_i, and pQ_i is the projection of the vector pq_i onto the plane S. Then the relation between normal curvature and principal curvature is according to Euler's formula

$$k_n^i = k_1 cos^2(\theta_i + \theta) + k_2 sin^2(\theta_i + \theta) \quad , i = 1, 2 \dots, m. \tag{6}$$

The task can be written as an optimization problem.

$$\min_{k_1, k_2, \theta} \sum_{i=1}^{m} [k_1 cos^2(\theta_i + \theta) + k_2 sin^2(\theta_i + \theta) - k_n^i]^2 \tag{7}$$

After least squares, the principal curvatures k_1 and k_2 can be deduced as eigenvalues of the matrix W. $W = \begin{bmatrix} k_1 cos^2\theta + k_2 sin^2\theta & (k_2 - k_1)cos\theta sin\theta \\ (k_2 - k_1)cos\theta sin\theta & k_1 sin^2\theta + k_2 cos^2\theta \end{bmatrix}$. Then the point p Gaussian curvature k is

$$k = k_1 k_2. \tag{8}$$

C. Correspondence and Transformation Estimation based on Improved GeoTransformer

In order to perform better in plant point cloud alignment scenarios with distinct curvature features, we embedded the geometric structure encoding containing the pair-wise distances, triplet-wise angles, and point curvatures based on neighboring point normal vector estimation into the geometric self-attention module of the Superpoint Matching module of GeoTransformer's backbone, and then utilized the improved GeoTransformer to perform the point cloud matching, which in turn acquired the corresponding and transformation estimation of the point cloud alignment scenarios of plants with low overlap rate $T = \{R, t\}$.

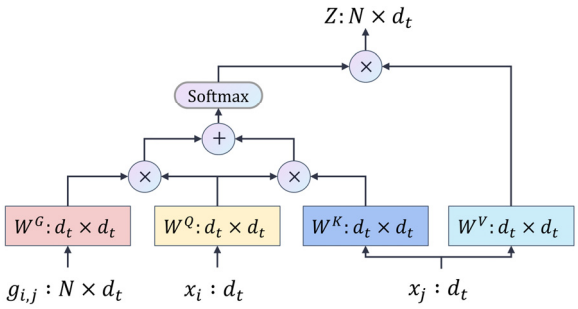

Figure 5. Geometric structure coding embedded in geometric self-attention module

The geometric structure encoding is embedded into the geometric self-attention module as shown in Fig. 5, corresponding to equation (10):

$$\begin{cases} e_{i,j} = \dfrac{(x_i W^Q)(x_j W^K + g_{i,j} W^G)^T}{\sqrt{d_t}} \\ z_i = \sum_{j=1}^{P} a_{i,j}(x_j W^V) \end{cases}, \tag{9}$$

where $e_{i,j}$ is the geometric self-attention score, x_i, x_j are the contextual features of points p_i, p_j outputted by the Feature Extraction module of GeoTransformer, d_t is the dimension of the features, and W^Q, W^K, W^V, $W^G \in R^{d_t \times d_t}$ are the projection matrices of queries, keys, values and geometric structure respectively; $a_{i,j}$ is the score of $e_{i,j}$ normalized by softmax, and z_i is the feature of point p_i output by the geometric self-attention module.

III. EXPERIMENTS

A. Environment

The programming environment uses Python 3.8 as the development language, using Pycharm 2022.2 integrated development editors, using the PyTorch deep learning framework. All models are trained in a server (two NVIDIA GeForce RTX 2080 Ti 12GB), accelerated with deep neural network training using CUDA 10.2 and cuDNN 8.3, with Intel® Core™ i9-10900X with 6 core CPU, and Ubuntu 20.04 operating system.

B. Performance

In this paper, three commonly used evaluation metrics for point cloud alignment: (1) Relative Rotation Error (RRE), the geodesic distance between estimated and ground-truth rotation matrices, (2) Relative Translation Error (RTE), the Euclidean distance between estimated and ground-truth translation vectors, (3) Root Mean Square Error (RMSE), are used to evaluate the effectiveness of the point cloud alignment of the model. The formulas are

$$RRE = \cos^{-1}\left(\frac{1}{2}trance(est_{\text{rotation}} \cdot gt_{\text{rotation}} - 1)\right), \quad (10)$$

$$RTE = \| est_{\text{translation}} - gt_{\text{translation}} \|_2, \quad (11)$$

$$RMSE = \sqrt{\frac{\| gt_{\text{points}} - est_{\text{points}} \|_2}{M}}, \quad (12)$$

where est_{rotation} and $est_{\text{translation}}$ are rotation matrix and translation vector estimated by the model, gt_{rotation} and $gt_{\text{translation}}$ are the rotation matrix and translation vector of ground_true aligned by the FARO SCENE 3D point cloud software, trance is the tracing function. And gt_{points}, est_{points} are the point clouds after applying ground_true transform and estimation transform to the source point cloud, respectively.

The performance of the point cloud registration shown in Fig. 6d–f and 7d–f is listed in Table II and Table III. It can be seen that the errors of ICP in overlap rate #3 to #5, and #8 to #10 are large, which is consistent with Fig. 6 and Fig. 7. This indicates that the traditional method ICP is more dependent on the overlap rate of the point cloud and is less effective in point cloud alignment with low overlap rate. For the recent advanced deep learning point cloud registration methods focusing on low overlap rates (Predator and GeoTransformer) and the proposed methods perform better in overlap rates #3 to #5 and #8 to #10.

Further, the RMSE errors of the proposed method are only 1.7%, 6%, and 51% of ICP, Predator, and GeoTransformer, respectively, in overlap rate #5 for plant 1 and the mean of the errors in overlap rate #1 to #5 for plant 1 are only 1.7%, 6%, and 51% of ICP, Predator, and GeoTransformer, respectively, in overlap rate #1 to #5, 1.9%, 8%, and 33.7% of GeoTransformer. Similarly, the RMSE errors of the proposed method are only 1.8%, 25.7%, and 28.2% of ICP, Predator, and GeoTransformer for overlap rate #5 for plant 2 and the mean value of the errors for overlap rate #1 to #5 for plant 1 are only 1.9%, 25.7%, and 28.2% of ICP, Predator, and GeoTransformer, respectively, GeoTransformer's 3.8%, 28.7%, and 49.5%. The proposed method, with higher rates of success and accuracy, outperforms the other three methods.

TABLE II. REGISTRATION PERFORMANCE OF PLANT-1

Part I of Plant-1						
Overlap Number	**ICP**			**Predator**		
	RRE(°)	***RTE(cm)***	***RMSE(cm)***	***RRE(°)***	***RTE(cm)***	***RMSE(cm)***
#1	0.80	0.01	0.56	1.48	0.12	1.56
#2	2.60	0.21	3.60	3.67	0.32	1.58
#3	2.53	0.27	14.41	1.45	0.11	1.64
#4	10.71	0.16	27.37	8.32	0.15	4.51
#5	43.57	3.22	32.21	11.90	1.25	9.03
Mean	12.04	0.77	15.63	5.36	0.39	3.66
Part II of Plant-1						
Overlap Number	**GeoTransformer**			**Ours**		
	RRE(°)	***RTE(cm)***	***RMSE(cm)***	***RRE(°)***	***RTE(cm)***	***RMSE(cm)***
#1	1.21	0.10	0.72	0.25	0.02	0.14
#2	1.18	0.05	0.73	0.35	0.02	0.22
#3	1.33	0.06	0.85	0.26	0.01	0.24
#4	0.44	0.05	0.90	0.09	0.01	0.28
#5	1.58	0.15	1.08	0.73	0.05	0.55
Mean	1.15	0.08	0.86	0.34	0.02	0.29

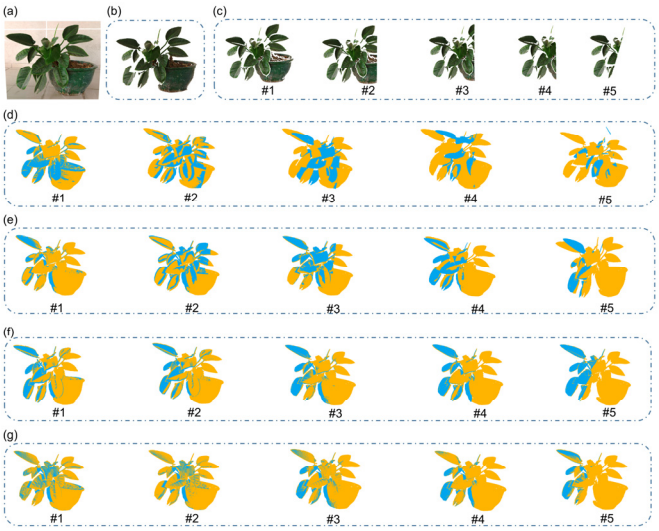

figure 6. The inputs and the registration results of plant-1: (a) the actual scene photo of plant -1; (b) target point cloud; (c) source point clouds with different overlap rates than the target point cloud ; (d–f) registration results of ICP, Predator, GeoTransformer, and the proposed method, respectively. Point cloud overlap rates are numbered from #1 to #5.

figure 7. The inputs and the registration results of plant-2: (a) the actual scene photo of plant -2; (b) target point cloud; (c) source point clouds with different overlap rates than the target point cloud ; (d–f) registration results of ICP, Predator, GeoTransformer, and the proposed method, respectively. Point cloud overlap rates are numbered from #6 to #10.

TABLE III. REGISTRATION PERFORMANCE OF PLANT-2

Part I of Plant-2						
Overlap Number	**ICP**			**Predator**		
	RRE(°)	***RTE(cm)***	***RMSE(cm)***	***RRE(°)***	***RTE(cm)***	***RMSE(cm)***
#6	0.06	1.99	0.98	2.48	0.88	0.85
#7	0.14	2.16	1.56	2.71	1.04	1.55
#8	0.36	3.96	5.65	1.63	0.75	1.86
#9	46.55	13.88	18.03	2.63	2.14	2.10
#10	99.54	63.23	44.01	4.35	1.62	3.04
Mean	29.33	17.04	14.05	2.76	1.29	1.88
Part II of Plant-2						
Overlap Number	**GeoTransformer**			**Ours**		
	RRE(°)	***RTE(cm)***	***RMSE(cm)***	***RRE(°)***	***RTE(cm)***	***RMSE(cm)***
#6	0.09	0.03	0.28	0.14	0.15	0.43
#7	0.19	0.22	0.38	0.21	0.24	0.47
#8	0.59	0.35	0.86	0.26	0.26	0.50
#9	1.14	0.13	1.20	0.35	0.28	0.53
#10	5.10	1.89	2.77	1.19	0.39	0.78
Mean	1.42	0.52	1.09	0.43	0.26	0.54

IV. CONCLUSION

In order to achieve point cloud alignment in crop point clouds with low overlap rates, an improved GeoTransformer point cloud registration method based on Gaussian curvature estimated from neighboring point normal vectors is developed in this study. Encoded point cloud geometric features, including pair-wise distances, triplet-wise angles, and point curvatures estimated based on normal vectors of neighboring points, are embedded into the GeoTransformer module through a Self-Attention Mechanism to achieve point cloud correspondence and transformation estimation. The method is rotationally invariant and suitable for crop point cloud registration with low overlap rate, and its validity is verified on real-world collected crop point clouds with low overlap rate, and its success rate and accuracy are also superior to ICP, Predator, and GeoTransformer methods. It can effectively extract the phenotypic features of plants, and has important practical application value in the field of agriculture. The future work focuses on optimizing the memory occupation of the data and expanding to large-scale crop point cloud alignment scenarios.

ACKNOWLEDGMENT

This work is financially supported by Collaborative Education Project of Ministry of Education with Beijing Piesat Information Technology Co.Ltd (220802313160749), Guangzhou Fundamental and Applied Research Grant (202201010273), and General Program of Natural Science Foundation of Guangdong Province.

REFERENCES

[1] Huang, Xiaoshui, et al. "A comprehensive survey on point cloud registration." *arXiv preprint arXiv:2103.02690* (2021).

[2] Peng, Yeping, et al. "Point Cloud Registration Based on Fast Point Feature Histogram Descriptors for 3D Reconstruction of Trees." *Remote Sensing* 15.15 (2023): 3775.

[3] Liu, Yadong, et al. "Fast reconstruction method of three-dimension model based on dual RGB-D cameras for peanut plant." *Plant Methods* 19.1 (2023): 17.

[4] XIE Zhonghong, HUANG Yifan, WU Chongyou. Point cloud registration method of rape branches based on ISS-LCG combined feature points[J]. Journal of South China Agricultural University,2023,44(3):456-463.

[5] Zhu, Tianyu, et al. "A calculation method of phenotypic traits based on three-dimensional reconstruction of tomato canopy." *Computers and Electronics in Agriculture* 204 (2023): 107515.

[6] Zhang, Zhengyou . "Iterative Closest Point (ICP)." Springer US (2014).

[7] Huang, Shengyu, et al. "Predator: Registration of 3d point clouds with low overlap." *Proceedings of the IEEE/CVF Conference on computer vision and pattern recognition*. 2021.

[8] Qin, Zheng, et al. "GeoTransformer: Fast and Robust Point Cloud Registration With Geometric Transformer." *IEEE Transactions on Pattern Analysis and Machine Intelligence* (2023).

[9] Zhang, Xiaopeng, Hongjun Li, and Zhanglin Cheng. "Curvature estimation of 3D point cloud surfaces through the fitting of normal section curvatures." *Proc. AsiaGraph* (2008): 72-79.

[10] Han, Kai, et al. "A survey on vision transformer." *IEEE transactions on pattern analysis and machine intelligence* 45.1 (2022): 87-110.